Research Paper

Inhibition of Lymphangiogenesis of Endothelial Progenitor Cells with VEGFR-3 siRNA Delivered with PEI-alginate Nanoparticles

Ting Li, Guo-dong Wang, Yu-zhen Tan, Hai-jie Wang ✉

Department of Anatomy, Histology and Embryology, Shanghai Medical School of Fudan University, Shanghai 200032, China

✉ Corresponding author: Hai-jie Wang Professor, MD., PhD., Department of Anatomy, Histology and Embryology, Shanghai Medical School of Fudan University, 277# 138 Yixueyuan Road, Shanghai 200032, People's Republic of China. Tel: +86-21-54237430; Fax: +86-21-54237430; E-mail: hjwang@shmu.edu.cn

Abstract

Lymphangiogenesis is implicated in lymphatic metastasis of tumor cells. Recently, growing evidences show that endothelial progenitor cells (EPCs) are involved in lymphangiogenesis. This study has investigated effects of VEGF-C/VEGFR-3 (vascular endothelial growth factor receptor-3) signaling pathway on EPC differentiation and effectiveness of inhibiting lymphatic formation of EPCs with VEGFR-3 siRNA delivered in PEI (polyethylenimine)-alginate nanoparticles. CD34$^+$VEGFR-3$^+$ EPCs were sorted from mononuclear cells of human cord blood. Under induction with VEGF-C, the cells differentiated toward lymphatic endothelial cells. The nanoparticles were formulated with 25 kDa branched PEI and alginate. The size and surface charge of PEI-alginate nanoparticles loading VEGFR-3 siRNA (N/P = 16) are 139.1 nm and 7.56 mV respectively. VEGFR-3 siRNA specifically inhibited expression of VEGFR-3 mRNA in the cells. After treatment with PEI-alginate/siRNA nanocomplexes, EPCs could not differentiate into lymphatic endothelial cells, and proliferation, migration and lymphatic formation of EPC-derived cells were suppressed significantly. These results demonstrate that VEGFR-3 signaling plays an important role in differentiation of CD34$^+$VEGFR-3$^+$ EPCs. VEGFR-3 siRNA delivered with PEI-alginate nanoparticles can effectively inhibit differentiation and lymphangiogenesis of EPCs. Inhibiting VEGFR-3 signaling with siRNA/nanocomplexes would be a potential therapy for suppression of tumor lymphangiogenesis and lymphatic metastasis.

Key words: VEGFR-3, endothelial progenitor cells, nanoparticles, polyethyleneimine, alginate.

Introduction

Lymphangiogenesis, the formation of new lymphatic vessels from the preexisted ones, undergoes proliferation, migration and tube formation of the lymphatic endothelial cells [1, 2]. Growth factors, adhesion molecules, chemokines and extracellular matrix play important roles in lymphangiogenesis [3–5]. In comparison with blood capillaries, lymphatic capillaries begin as the dilated lymphatics with the closed ends, and lack continuous basement membrane. There are discontinuous button-like junctions between lymphatic endothelial cells. The cells are tethered to the surrounding bundles of collagen by anchoring filaments regulating the valve-like opening into the lymphatic vessel lumen. The lymphatic endothelium expresses Prox-1, podoplanin, and LYVE-1 (lymphatic vessel endothelial hyaluronan receptor-1). VEGFR-3 (vascular endothelial growth factor receptor-3) is mainly expressed on the lymphatic endothelium though its expression was observed on the endothelial cells of hepatic sinusoid and blood vessels in

tumor. Lymphatic vessels drain excess fluid from the extracellular spaces, absorb lipids from the intestine, and transport leukocytes and antigen-presenting cells from inflammatory tissue to lymph nodes. Therefore, lymphatic vessels contribute to pathogenesis of various diseases involving immune and inflammatory responses and its role in disseminating tumor cells [6, 7]. Recent intense studies show important clinical implication of lymphangiogenesis in tumors and inflammatory diseases [6, 8]. Lymphangiogenesis under these pathological environments may result in tumor metastasis and graft rejection.

Lymphvasculogenesis, another form of new lymphatic vessel formation, is involved in development of the lymphatic vasculature. During early stages of development, Prox-1+ cells migrated from the jugular veins express VEGFR-3 and LYVE-1, and differentiate toward lymphatic endothelial cells to form the primary lymphatic vessels [9]. Under induction with VEGF-C and VEGF-A, embryonic stem cells may differentiate to form lymphatic vessel structures [10]. Recent growing evidences show that lymphatic endothelial progenitor cells (LEPCs) contribute to postnatal lymphangiogenesis. A population of CD34+ lymphatic/vascular endothelial precursor cells has been identified in human fetal liver, cord and periphery blood [11]. In patients with small cell lung cancer, VEGFR-3-positive circulating lymphatic/vascular endothelial progenitor cells increase [12]. Some CD34+ EPC-derived cells become positive for LYVE-1 after stimulation with growth factors [13]. EPCs are capable of incorporating into the endothelium of the growing lymphatic vessels in the cornea of mouse treated with irradiation [14] and the transplanted human kidney [15]. Moreover, EPCs differentiating towards lymphatic endothelial cells were observed at the microvessels of mouse lung [16]. Main biomarkers of LEPCs are expression of CD34, CD133 and VEGFR-3. Under induction with VEGF-C, the cells can differentiate into lymphatic endothelial cells via VEGFR-3 signaling. In postnatal lymphangiogenesis, LEPCs may be mobilized from bone marrow to peripheral blood, transmigrate through blood capillaries to home to the local tissue, and differentiate towards lymphatic endothelial cells that participate in formation of new lymphatic vessels.

Inhibition of lymphangiogenesis may be a powerful selective therapy for reducing lymphatic metastasis of tumor cells. RNA interference (RNAi) is the process of sequence-specific post-transcriptional gene silencing triggered by double-stranded small interfering RNA (siRNA) composed of 21–25 nucleotides. Compared with small molecule inhibitors and monoclonal antibodies, the key therapeutic advantage of RNAi lies in its ability to specifically and potently knock down the expression of disease-causing genes of known sequence [17]. Naked siRNA is unstable owing to nucleases in serum and cellular compartments and rapid renal clearance, leading to degradation and a short half-life. Interestingly, nanoparticles hold promise for the safe and effective intracellular delivery of siRNA [18]. Recently, more and more attention has focused on exploring antiangiogenic cancer gene therapy. Systemic administration of VEGF siRNA [19] or VEGFR-2 siRNA [20] in sterically stabilized nanoparticles may effectively inhibit angiogenesis and growth of tumors. It is well established that VEGFR-3 is a specific receptor of VEGF-C and VEGF-D. Upregulation of expression of VEGF-C and VEGF-D in tumor cells promotes tumor lymphangiogenesis and metastasis [8]. However, inhibiting VEGF-C/VEGFR-3 or VEGF-D/VEGFR-3 signaling pathway for supressing tumor lymphangiogenesis with siRNA delivered in nanoparticles remains unknown.

This investigation is designed to determine feasibility of VEGFR-3 siRNA delivery using alginate-modified polyethyleneimine (PEI) nanoparticles for inhibiting LEPC-induced lymphangiogenesis. CD34+VEGFR-3+ EPCs were isolated from mononuclear cells of human cord blood. VEGFR-3 siRNA-loaded PEI-alginate nanoparticles were characterized by dynamic light scattering and scanning and transmission electron microscopies. Toxicity and degradation of the nanoparticles in the cells were examined. After VEGFR-3 siRNA was delivered with PEI-alginate nanoparticles into the cells, inhibition of proliferation, migration and tube formation of the cells in matrix were evaluated.

Materials and methods

Isolation of EPCs

Human umbilical cord blood was collected from placentas of healthy delivery women. This study was approved by Ethics Committee of Shanghai Health Hospital for Women and Children, the informed consents were obtained from parents of newborns. Heparin (1×10^3 IU) was added into blood for preventing clotting. After blood was placed at room temperature for 30 min, mononuclear cells were isolated by density-gradient centrifugation (× 800 g, 30 min) with 1.076 Percoll solution (Amersham Pharmacia Biotech, Sweden) [21]. The cells were suspended in Dulbecco's modified Eagle's medium (DMEM; Invitrogen, NE, USA) supplemented with 10% fetal bovine serum (FBS; Gibco Invitrogen, NY, USA), 100 U/ml penicillin and 100 µg/ml streptomycin, and seeded into culture dishes pre-coated with gelatin (Sigma, CA, USA) at a density of 1×10^6 cells/ml. Af-

ter incubation in a humidified incubator containing 5% CO_2 at 37°C for 24 h, non-adhered cells were removed by washing with PBS. The adhered mononuclear cells were harvested with digestion in 0.25% trypsin-EDTA (Gibco Invitrogen, NY, USA), density of the cells was adjusted to 1×10^7 cells/ml with the medium.

The mononuclear cells were incubated with mouse anti-human CD34 antibody (1:100; Diagnostica, NJ, USA) and rabbit anti-human VEGFR-3 antibody (1:100; Santa Cruz Biotechnology, CA, USA), or mouse anti-human CD133 antibody (1:100; Diagnostica, NJ, USA) and rabbit anti-human VEGFR-3 antibody (1:100) at 4°C for 50 min. Nonspecific antigen of the cells was blocked with 5% bovine serum albumin (BSA; GE Healthcare, London, UK). After rinsing with PBS containing 1% BSA, the cells were incubated with goat anti-mouse cy3-IgG (1:200) and goat anti-rabbit FITC-IgG (1:200; Chemicon, CA, USA) at 4°C for 30 min. Following washing with PBS, the cells were suspended with DMEM supplemented with 2.5% FBS [22]. In the control group, the cells were only incubated with the second antibody. CD34+/VEGFR-3+ cells or CD133+/VEGFR-3+ cells were analyzed, and CD34+/VEGFR-3+ cells were sorted by a Beckman MoFlo™ XDP FACS (Beckman Coulter, CA, USA). The cells were collected in DMEM containing 20% FBS, 100 U/ml penicillin and 100 μg/ml streptomycin. After counterstaining with 4',6-Diamidino-2-phenylindole (DAPI, 1:1000; Sigma), the coexpression of CD34 or CD133 and VEGFR-3 was examined with a confocal laser scanning microscope (Carl Zeiss, Oberkochen, Germany). For expansion, the sorted cells were incubated with the medium supplemented with 50 ng/ml VEGF-C (Sigma, CA, USA) [23]. For identification of cell differentiation, the cells induced with VEGF-C for two weeks were incubated with rabbit anti-human LYVE-1 antibody (1:100; AngioBio, CA, USA) overnight at 4°C. After washing, the cells were incubated with FITC-labeled goat anti-rabbit IgG (1:300; Jackson ImmunoResearch Laboratories, PA, USA) for 30 min at 37°C. The nuclei were counterstained with DAPI. The cells were viewed using a fluorescence microscope.

Formulation of PEI-alginate nanoparticles

PEI-alginate nanoparticles were fabricated according to Patnaik's method [24] with minor modification. The positive charge of 25 kDa branched PEI (Sigma, CA, USA) was partially neutralized by electrostatic interaction with alginate (Sigma, CA, USA). Briefly, PEI and alginate were dissolved in the heated distilled water respectively, and then the solutions were filtered with a syringe filter (0.22 μm; Millipore, Shanghai, China). Alginate solution was added to PEI

solution, their proportion is 4.8%. The mixed solution was incubated for 30 min at room temperature. PEI-alginate nanoparticle solution was stored at 4°C before use.

Determination of siRNA loading efficiency

VEGFR-3 siRNAs (Table 1) were designed and synthetized by GenePharma (Shanghai, China). The siRNA (1 μg) was dropped to PEI-alginate nanoparticle solution at different N/P ratios. According to weight of nitrogen in the PEI and phosphorus in the siRNA, N/P ratio was calculated with the equation: N/P ratio = 7.75 × PEI (μg)/siRNA (μg). For formation of PEI-alginate/siRNA nanocomplexes, the suspension was vibrated gently and incubated for 30 min at room temperature. For determining siRNA loading efficiency, the nanocomplexes were mixed with loading buffer containing tracking dye (bromphenol blue, 1:9). The mixed liquor was added into the well of 1% agarose gel and electrophoresed at 100 V for 30 min in Tris-acetate-EDTA buffer (pH 8.3) containing ethidium bromide. The bands binding to the siRNA were visualized under a UV transilluminator at a wavelength of 365 nm, the images were analyzed with a software (Furi Science & Technology, Shanghai, China). The size and zeta potential of the nanocomplexes were measured using a dynamic light scatter (Santa Barbara, CA, USA). The results of nanocomplex measurement were compared with that of the PEI-alginate nanoparticles without siRNA.

Table 1. Sequences of VEGFR-3 siRNAs.

VEGFR3-homo-3826 (No. 1)	Sense: 5'-CCAGGAUGAAGACAUUUGATT-3'
	Antisense: 5'-UCAAAUGUCUUCAUCCUGGTT-3'
VEGFR3-homo-2457 (No. 2)	Sense: 5'-CUCCUCAUCUUCUGUAACATT-3'
	Antisense: 5'-UGUUACAGAAGAUGAGGAGTT-3'
VEGFR3-homo-483 (No. 3)	Sense: 5'-GAGCAGCCAUUCAUCAACATT-3'
	Antisense: 5'-UGUUGAUGAAUGGCUGCUCTT-3'
Negative control siRNA	Sense: 5'-UUCUCCGAACGUGUCACGUTT-3'
	Antisense: 5'-ACGUGACACGUUCGGAGAAAT-3'

Cell transfection with VEGFR-3 siRNA

For detecting transfection of siRNA loaded with PEI-alginate nanoparticles into the cells, siRNA was labeled with 5-carboxyfluorescein (Sigma, CA, USA). The sorted EPCs were seeded in 24-well culture plate

at a density of 1×10^5 cells/well and incubated for 24 h. The nanocomplexes containing siRNA or negative control FAM-siRNA (Table 1) were diluted with serum-free DMEM as transfection solution. After treatment with transfection solution for 4 h, the solution was replaced with fresh complete medium, the cells continued to be incubated for 48 h [25]. The cells transfected by siRNA labeled with FAM were examined with a fluorescence microscopy. The experiment was repeated at least thrice. Efficacy of transfection was evaluated as number of the positive cells. For selecting the most effective VEGFR-3 siRNA, the cells were transfected with three synthesized siRNAs respectively with same method above.

Cytotoxicity assay of nanocomplexes with different N/P ratios

Cytotoxicity of PEI-alginate/siRNA nanocomplexes was examined by MTT (methylthiazolyldiphenyl-tetrazolium bromide; Sigma, CA, USA) assay. The cells were seeded in 96-well plate at density of 5×10^3 cells (150 µl medium). After incubation for 24 h, the cells were treated with the nanocomplexes containing negative control siRNA with different N/P ratios for 4 h. Then, the medium was replaced, the cells continued to be incubated for 20 h. The cells treated with PEI/siRNA complexes were taken as the control. After adding of MTT solution (5 mg/ml), the cells were incubated for 4 h. Following removal of the medium containing MTT, 150 µl dimethylsulfoxide (DMSO; Sigma, CA, USA) was added to dissolve formazan crystal formed by live cells. The absorbance was measured at 540 nm with an absorbance microplate reader (BIO-RAD, Hercules, CA, USA). The assay was repeated thrice. Cell viability was calculated by the equation: cell viability (%) = [OD_{540} (sample)/OD_{540} (control)] × 100%. Changes of cell viability in PEI-alginate/siRNA group were compared with PEI/siRNA group.

RT-PCR assay

For selecting the most effective siRNA in interfering expression of VEGFR-3 gene, expression of VEGFR-3 mRNA in the cells transfected with different siRNAs was examined with semi-quantitative reverse transcription-PCR (RT-PCR) using a one-step RT-PCR kit (BestBio, Shanghai, China). Preparation of PEI-alginate/siRNA nanocomplexes (N/P = 16) and transfection of the cells were performed as above. Total RNA of the cells was extracted using TRIzol reagent (Invitrogen, NE, USA) as the manufacturer's protocol. The mRNA levels were normalized using GAPDH as a housekeeping gene. RT-PCR was carried out as the following thermal cycling conditions: cDNA synthesis; 1 cycle 55°C for 30 min,

denaturation; 1 cycle 94°C for 2 min, PCR amplification; 35 cycles at 94°C for 60 s, at 60°C for 60 s, and at 65°C for 60 s, final extension; 1 cycle 65°C for 10 min. The PCR primers for detecting human VEGFR-3 (forward: 5′-AGCCATTCATCAACAAGCCT-3′, reverse: 5′-GGCAACAGCTGGATGTCATA-3′) and human GAPDH (forward: 5′-TGAAGGTCGGAGTCAACGGATTTGGT-3′, reverse: 5′-CATGTGGGCCATGAGGTCCACCAC-3′) were synthesized by Sangon Biotech (Shanghai, China). The sizes of the PCR products for VEGFR-3 and human GAPDH were 298 bp and 983 bp respectively. The PCR products were separated in a 1% agarose gel by electrophoresis and visualized by staining with ethidium bromide. The images were analyzed by gel image analysis system (Furi Science & Technology, Shanghai, China). The most effective siRNA (VEGFR-3 siRNA #1; Table 1) was used in the following experiment of VEGFR-3 mRNA inhibition.

Scanning and transmission electron microscopy

The cells were seeded on coverslips and treated with PEI-alginate nanoparticles loading VEGFR-3 siRNA for 2 h. Then, the cells were fixed with 2.5% glutaraldehyde, dried under vacuum and coated with gold-palladium. Features of the nanocomplexes and phagocytosis of the nanocomplexes by the cells were examined with a scanning electron microscopy (FEI QUANTA200, Philips, DA Best, The Netherlands).

For examining degradation of the nanocomplexes, the cells on coverslips were treated with the nanocomplexes for 2 h, 4 h and 6 h respectively. The cells obtained *in situ* were fixed with 2.5% glutaraldehyde at 4°C, and then with l% osmium tetroxide. After being dehydrated with gradient alcohol, soaked with anhydrous acetone and Spurr resin, the cells were embedded with Spurr resin. Ultrathin sections were prepared with Reichert-ultracut E ultrathin microtome (Leica, St. Gallen, Switzerland), and then stained with 3% uranyl acetate and lead citrate [26]. The distribution of the nanocomposites in the cells was viewed by a CM120 transmission electron microscope (Philips, Eindhoven, Holland). Degradation of the nanocomposites was examined.

Detection of cell viability

Viability of the cells treated with PEI-alginate/siRNA nanocomplexes (N/P = 16) was determined with MTT assay as above. After treatment with the nanocomplexes for 4 h, the medium was changed with fresh medium. Then, the cells were incubated for 12 h, 24 h, 36 h, 48 h, and 72 h respectively. The untreated cells were taken as control with 100% viability, the wells without addition of MTT were

used as blank to calibrate the spectrophotometer to zero absorbance.

PCNA staining

The cells were divided into control, VEGF-C, nanoparticle (without siRNA) and nanocomplex groups. In VEGF-C group, the cells were incubated with the medium supplemented with 50 ng/ml VEGF-C. In nanoparticle and nanocomplex groups, the cells under induction with VEGF-C were treated with the nanoparticles and nanocomplexes for 4 h respectively. Then, the medium was exchanged to remove excess nanoparticles or nanocomplexes, and the cells continued to be incubated with the medium supplemented with 50 ng/ml VEGF-C for 20 h. The cells were fixed with 4% paraformaldehyde for 30 min, and then treated with 30% hydrogen peroxide and 100% methanol (1:5) for 30 min to inactivate endogenic peroxidase. Heterogenetic antigen in the cells was blocked with BSA. Subsequently, the cells were incubated with PCNA (proliferating cell nuclear antigen) IgG2a (1:100; Boster Bio, Wuhan, China) overnight at 4°C, and then incubated with cy3-labeled goat anti-mouse IgG (1:100) for 20 min at 37°C. PCNA presents in the early G_1 and S phases of the cell cycle and serves as an excellent maker of proliferating cells [27]. The cells expressing PCNA were examined with a fluorescence microscope.

Migration assay

The cells were divided into four groups as above. In the nanocomplex group, the cells were treated with the nanocomplexes for 24 h and then collected with digestion in 0.25% trypsin-EDTA. The suspension of the cells (1 × 10^6 cells/ml) was added into the upper chamber of 12-well format of cell culture inserts (Becton Dickinson, France). In the lower chamber, the medium containing 50 ng/ml VEGF-C was added. Diameter of the pores in the membrane is 8 µm. After incubation for 24 h, the cells on the membrane were fixed with 100% methyl alcohol, and then stained with 10% Giemsa solution. The cells migrated into the lower chamber were counted using an optical microscope in five fields for each well. The experiment was repeated in triplicate.

Tube formation assay

The cells induced with 50 ng/ml VEGF-C for 10 days were used in this experiment. The cells were divided into four groups as above. In the nanocomplex group, the cells were treated with the nanocomplexes for 24 h and collected as above. Matrigel basement membrane matrix (BD Biosciences, NJ, USA) was diluted with serum-free DMEM (1:1). Matrigel matrix (0.5 ml/ well) was added into 24-well culture plate, and allowed to gel at 37°C for 10 min.

Then, the cells were seeded on the gel at density of 2 × 10^5 cells/well and incubated in the medium containing 50 ng/ml VEGF-C for 24 h. Capillary-like structures organized by the cells were viewed and photographed using a phase contrast microscope (Nikon, Japan). Five representative fields were selected randomly. Length and area of the structures were measured with Image-pro Plus 6.0 (Media Cybernetics, Silver Spring, MD, USA). The experiment was performed in triplicate.

Statistical analysis

All experiments were performed at least in triplicate. Data are expressed as the means ± standard deviation. To analyze the data statistically, Student's t-test and one-way analysis of variance with Scheffe's post hoc multiple-comparison analysis were performed. A value of $p < 0.05$ was considered to be statistically significant.

Results

Characteristics of CD34+VEGFR-3+ EPCs

In analysis with flow cytometry, number of CD34+VEGFR-3+ and CD133+VEGFR-3+ cells were 0.7% and 0.49% respectively in the mononuclear cells isolated from umbilical cord blood (Fig. 1A). The results of immunostaining showed that VEGFR-3+ cells expressed CD34 and CD133 (Fig. 1B). The fresh sorted CD34+VEGFR-3+ cells were round. At day 3 after induction with VEGF-C, some cells represented spindle-shape or polygon-shape. At day 7, the most cells are long spindle-shaped, and some cells proliferated into colonies (Fig. 1C). At day 14 after induction with VEGF-C, the cells expressed lymphatic endothelial maker LYVE-1 (Fig. 1D).

siRNA loading and cytotoxicity of the nanocomplexes

Gel retardation assay showed efficiency of siRNA loading in PEI-alginate nanoparticles increased following increase of N/P ratio. In our experiments, N/P ratio of PEI-alginate/siRNA nanocomplexes was determined 16 as desirable siRNA loading (Fig. 2A). The mean size and surface charge of PEI-alginate nanoparticles (N/P = 16) are 89.1 ± 55 nm and 9.04 ± 1.5 mV respectively. After loading with VEGFR-3 siRNA, the nanoparticles became larger (139.1 ± 70 nm), their surface charges decreased (7.56 ± 1.1 mV). Results of MTT assay showed that cell viability after treatment with the nanocomplexes decreased as N/P ratio increased. After treatment with nanoparticles for 24 h, cell viability is higher in PEI-alginate/siRNA group than PEI/siRNA group significantly. This result indicates that cytotoxicity of PEI-alginate nanoparticles is lower than PEI nanoparticles (Fig. 2B).

Expression of VEGFR-3 mRNA after VEGFR-3 siRNAs transfection

After transfection with VEGFR-3 siRNAs (Table 1) delivered with PEI-alginate nanoparticles for 4 h, the level of VEGFR-3 mRNA expression in the cells was examined with RT-PCR. In three VEGFR-3 siRNAs, VEGFR-3 siRNA #1 was most effective for inhibiting expression of VEGFR-3 mRNA in the cells (Fig. 3). The nanocomplexes loading VEGFR-3 siRNA #1 were applied in the experiments of inhibiting viability, proliferation, migration and tube formation the cells.

Uptake and degradation of the nanocomplexes
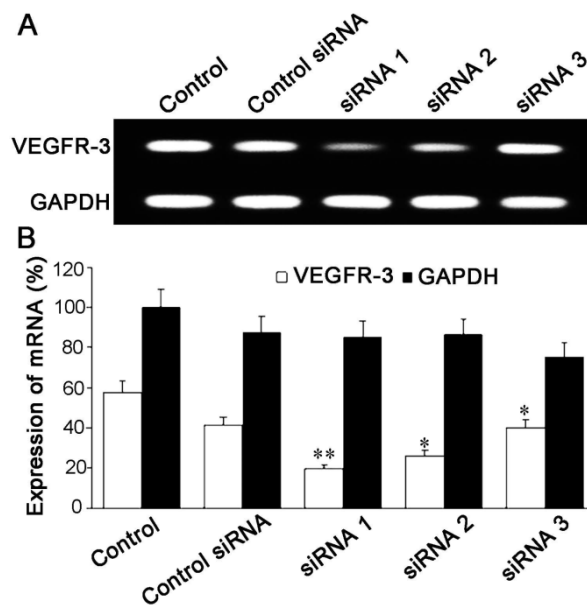
After exposing to PEI-alginate/siRNA nano-complexes for 2 h, the morphological characteristics of the cells phagocytizing the nanocomplexes were examined with scanning electron microscopy. Many round and smooth nanocomplexes adhered to cell membrane, some nanocomplexes were engulfed by the cells (Fig. 4A). Cup-like protrusion phagocytizing the nanocomplex was not observed. In examination with transmission electron microscope, some nanocomplexes were phagocytized into the cells after incubation for 2 h. At 4 h after incubation, the most nanocomplexes entered the cells. At 6 h, some nanocomplexes in the cells were degraded, and apoptotic cells were not found (Fig. 4B).
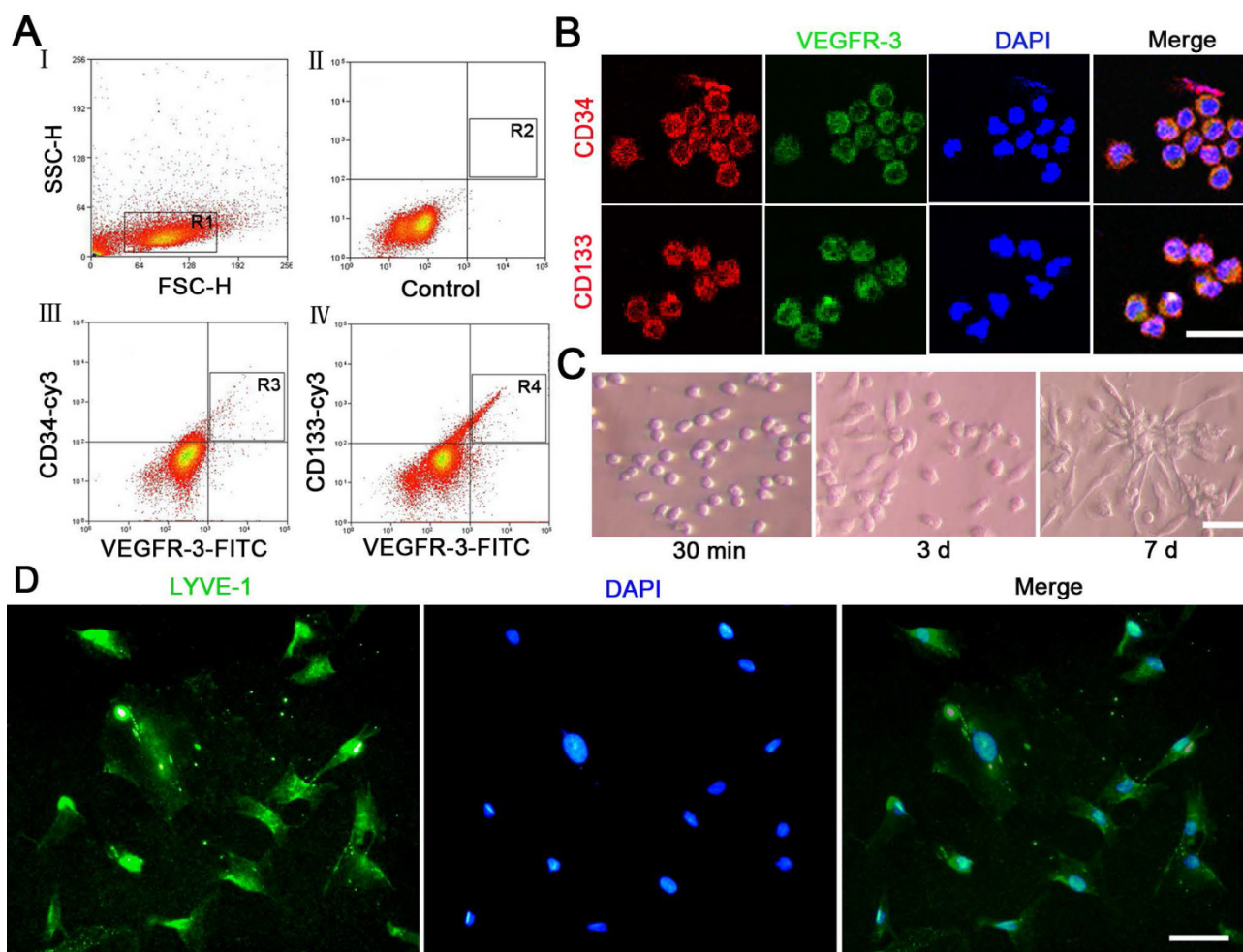

Fig. 1. Characteristics of CD34+VEGFR-3+ EPCs. (A) There are CD34+VEGFR-3+ cells and CD133+VEGFR-3+ cells in the mononuclear cells isolated from umbilical cord blood. The cells were analyzed with a flow cytometer. (B) In immunostaining, VEGFR-3+ cells express CD34 and CD133. (C) Features of CD34+VEGFR-3+ EPCs. After treatment with 50 ng/ml VEGF-C, the cells proliferate, the shape of the cells changes. (D) Expression of LYVE-1 on the differentiated cells. At day 14 after induction with VEGF-C, the cells are positive for LYVE-1 immunostaining. Bars = 25 μm.
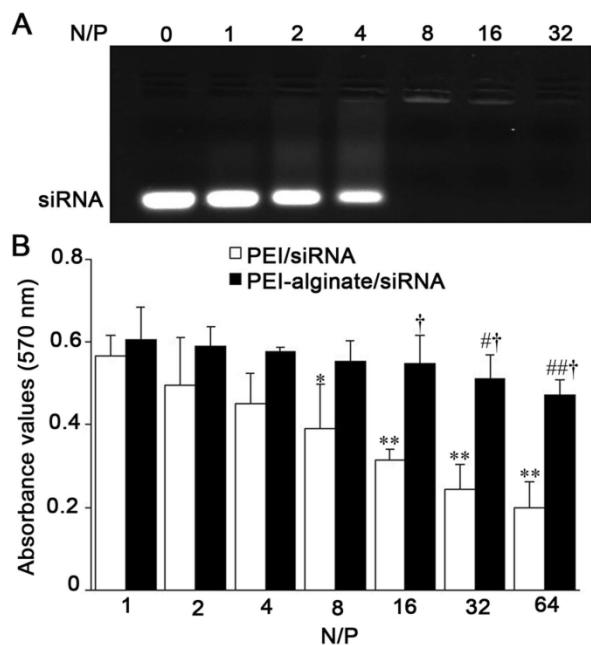
Fig. 2. Characteristics of PEI-alginate nanoparticles in loading VEGFR-3 siRNA. (A) siRNA loading in the nanoparticles. The negative control siRNA was loaded with the nanoparticles with different N/P ratios. It is desirable for siRNA loading that N/P ratio is 16. (B) Viability of the cells after treatment with the nanoparticles loading negative control siRNA with different N/P ratios. Cell viability was determined with MTT assay after treatment for 24 h. *$p < 0.05$, **$p < 0.01$ versus N/P ratio = 1 group (PEI/siRNA group); #$p < 0.05$, ##$p < 0.01$ versus N/P ratio = 1 group (PEI-alginate/siRNA group); †$p < 0.05$ versus PEI/siRNA group. n = 3.
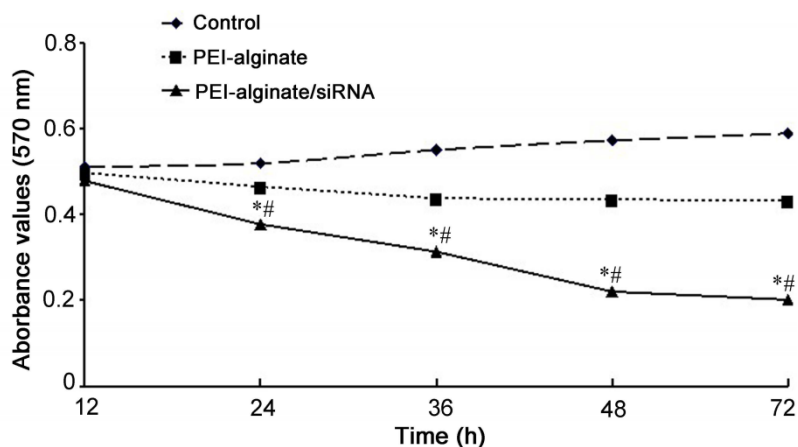
Fig. 3. Inhibition of VEGFR-3 mRNA expression after treatment with PEI-alginate/siRNA nanocomplexes. (A) Expression of VEGFR-3 mRNA. The cells were transfected with VEGFR-3 siRNA for 4 h. Inhibition of VEGFR-3 mRNA expression was analyzed with RT-PCR. Compared with VEGFR-3 siRNA #2 and VEGFR-3 siRNA #3, VEGFR-3 siRNA #1 inhibits expression of VEGFR-3 mRNA in the cells significantly. (B) Statistic results of VEGFR-3 mRNA expression. *$p < 0.05$, **$p < 0.01$ versus the control group. n = 5.
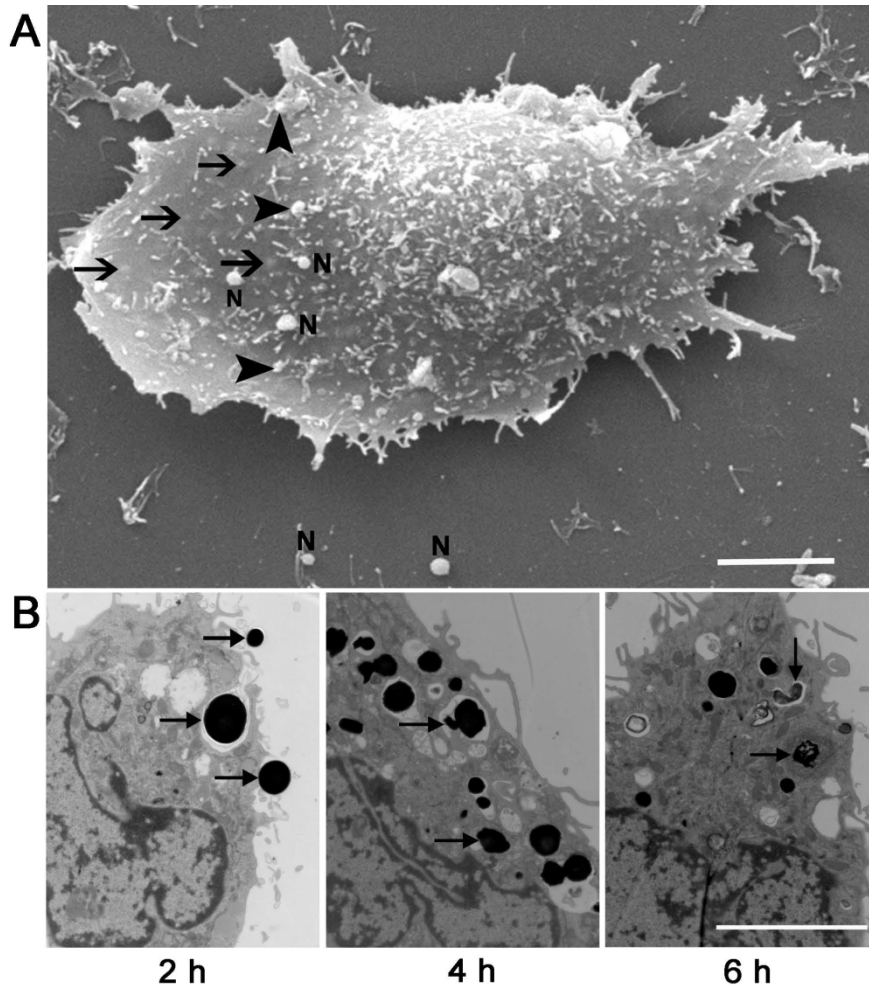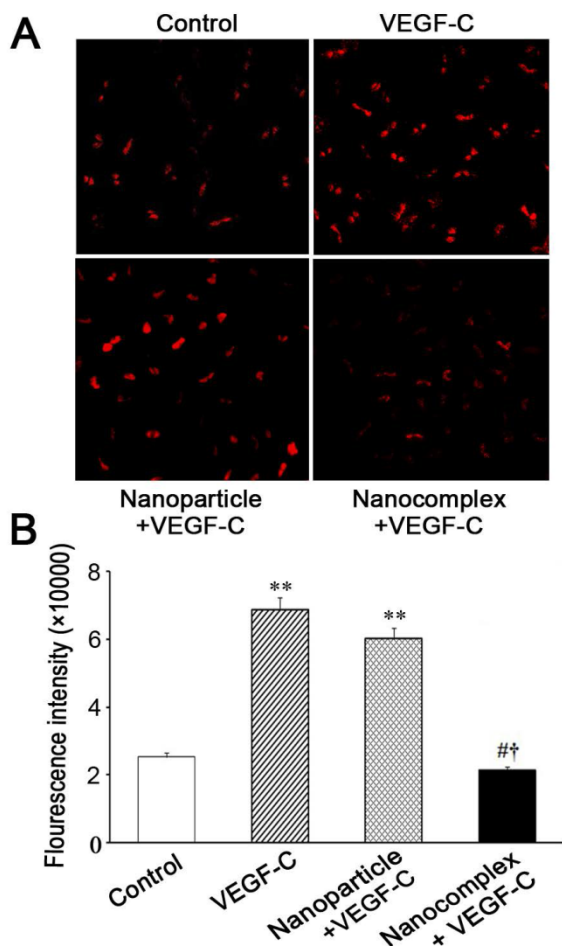
Fig. 4. Microphotographs of the cells treated with PEI-alginate/siRNA nanocomplexes. (A) Scanning electron microphotograph of the cell phagocytizing the nanocomplexes. Round nanocomplexes (arrowheads) adhere to cell membrane. Some nanocomplexes are phagocytized into the cell (arrows). N, free nanoparticle carrying siRNA. Bar = 2 μm. (B) Transmission electron microphotographs of the cells treated with the nanocomplexes. The nanocomplexes (arrows) are phagocytized into the cell after incubation for 2 h and 4 h. At 6 h, the nanocomplexes (arrows) in the cell are degraded. Bar = 1 μm.

Fig. 5. Viability of the cells after transfection with VEGFR-3 siRNA in PEI-alginate nanoparticles. Cell viability was analyzed with MTT assay. After treatment with PEI-alginate/siRNA nanocomplexes (N/P = 16), viability of the cells decreases significantly. $*p < 0.01$ versus control and PEI-alginate groups; $\#p < 0.05$ versus PEI-alginate group. n = 3.

Fig. 6. PCNA expression of the cells transfected with VEGFR-3 siRNA. (A) Microphotographs of PCNA expression in the cells. The cells were treated with PEI-alginate/siRNA nanocomplexes for 4 h. After removing excess nanocomplexes with medium exchange, the cells continued to be incubated for 20 h. Under VEGF-C induction, PCNA expression in the cells treated with the nanocomplexes decreases. Bar = 20 μm. (B) Statistic results of PCNA expression. The fluorescence density of the cells treated with the nanocomplexes decreases obviously. $**p < 0.01$ versus control group; $\#p < 0.01$ versus VEGF-C group; $\dagger p < 0.01$ versus nanoparticle group. n = 3.

Changes of cell viability after transfection of VEGFR-3 siRNA

The cells were treated with PEI-alginate nanoparticles or PEI-alginate/siRNA nanocomplexes (N/P = 16) for 4 h and then continued to be incubated for 12, 24, 36, 48 and 72 h respectively. Compared with PEI-alginate nanoparticle group, cell viability of PEI-alginate/siRNA nanocomplex group decreased. Differences in cell viability between control group and PEI-alginate nanoparticle group were not significant (Fig. 5).

Changes of cell proliferation after VEGFR-3 siRNA transfection

Under induction with VEGF-C, the cells were treated with PEI-alginate/siRNA nanocomplexes for 4 h. After the medium was exchanged, the cells continued to be incubated for 20 h. The cells were stained with anti-PCNA antibodies. PCNA expression of the cells increased after induction with VEGF-C. Compared with the VEGF-C and nanoparticle groups, PCNA expression of the cells in the nanocomplex group decreased significantly (Fig. 6).

Changes of cell migration after VEGFR-3 siRNA transfection

Under stimulation with VEGF-C, the cells in the upper chamber may migrate into the lower chamber through the pores of the membrane of the insert. After treatment with VEGF-C for 24 h, the migrated cells were examined. The migrated cells in the nanocomplex group were less significantly than ones in VEGF-C and nanoparticle groups (Fig. 7).

Tube formation of the cells after VEGFR-3 siRNA transfection

After incubation for 24 h, the cells could organized into capillary-like structures in Matrigel basement membrane matrix. Degree of tube formation of the cells was evaluated with length and area of the structures. In the nanocomplex group, tube formation was inhibited (Fig. 8). Compared with VEGF-C group, length and area of the tubes in nanocomplex group were less significantly (Table 2).

Table 2. Total length and area of capillary-like structures formed by the cells derived from CD34^{+}VEGFR-3^{+} EPCs.

Group	Length (mm/cm^2)	Area (mm^2/cm^2)
control	76.68 ± 6.82	4.80 ± 0.56
VEGF-C	188.9 ± 16.36*	12.86 ± 1.12*
Nanoparticle + VEGF-C	152.9 ± 16.36*	10.49 ± 1.33*
Nanocomplex + VEGF-C	63.86 ± 4.62#†	3.62 ± 0.78#†

*$p < 0.01$ vs the control group; #$p < 0.01$ vs VEGF-C group; †$p < 0.01$ vs nanoparticle group.
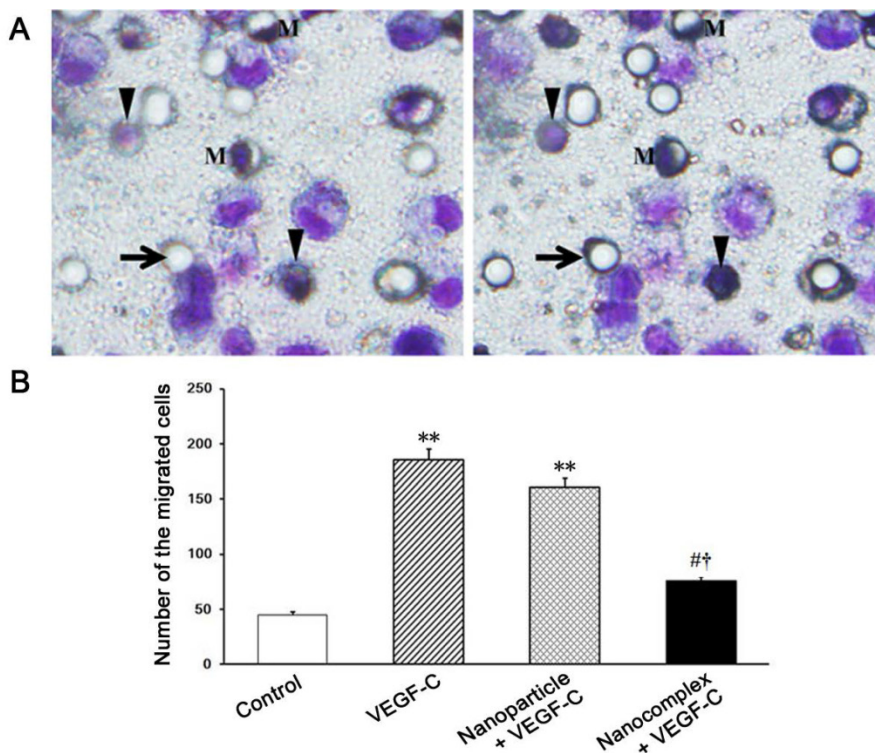
Fig. 7. Transmigration of the cells after treatment with PEI-alginate/siRNA nanocomplexes. The cells treated with the nanocomplexes for 24 h were seeded on the membrane of the insert, 50 ng/ml VEGF-C was added into the lower chamber. After incubation for 24 h, the cells on the membrane were stained with Giemsa solution, the migrated cells were counted. (A) Photographs of the cells on the membrane in the same field. The cells were focused in the upside (left graph) and underside (right graph) of the membrane respectively. Arrow, empty pore; Arrowhead, the cell migrated to underside of the membrane. M, the migrating cell through pore; Bar = 1 μm. (B) Statistic analysis of the migrated cells. In the nanocomplex group, the migrated cells are less. **$P < 0.01$ versus control; #$p < 0.05$ versus VEGF-C group; †$p < 0.05$ versus nanoparticle group.

Fig. 8. Capillary-like structures formed by the cells in Matrigel basement membrane matrix. The cells were treated with the nanocomplexes for 24 h and then seeded on the Matrigel in 24-well culture plate. The capillary-like structures formed by the cells in the nanocomplex group (D) are less than that in the control (A), VEGF-C (B) and nanoparticle (C) groups. Arrows indicate the tubes; Bar = 50 μm.
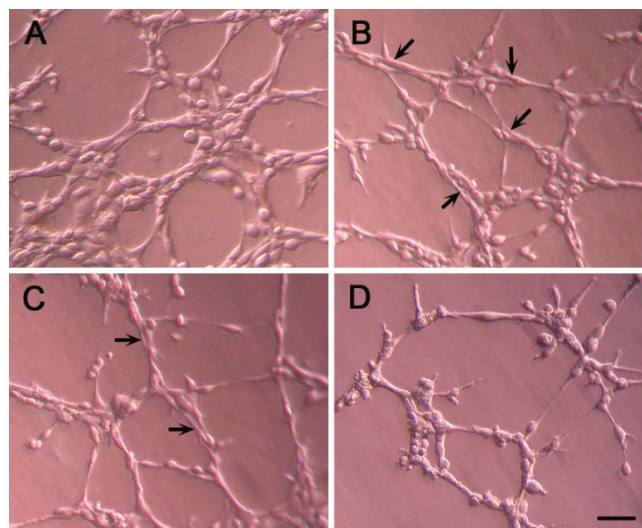
Discussion

The results of our experiments demonstrate that VEGFR-3 siRNA delivered with PEI-alginate nanoparticles inhibit significantly VEGF-C/VEGFR-3 signaling pathway in CD34$^+$VEGFR-3$^+$ EPCs. Under induction with VEGF-C, CD34$^+$VEGFR-3$^+$ cells sorted from mononuclear cells isolated from human umbilical cord blood have a potential to differentiate toward lymphatic endothelial cells and then form capillary-like structures in Matrigel matrix. After transfection of VEGFR-3 siRNA delivered in PEI-alginate nanoparticles, the cells can not differentiate into lymphatic endothelial cells, viability of the cells decreases. With inhibition of VEGFR-3 mRNA by VEGFR-3 siRNA loaded in PEI-alginate nanoparticles, lymphangiogenetic behaviors of the cells derived from CD34$^+$VEGFR-3$^+$ cells such as proliferation, migration and lymphatic formation are suppressed significantly. Therefore, VEGFR-3 may be regarded as a key biological marker of LEPCs. VEGF-C/VEGFR-3 and VEGF-D/VEGFR-3 signaling pathways play important roles in lymphangiogenesis under pathological conditions [28]. In graft mouse models, VEGF-C siRNA and VEGF-D siRNA transfected with lentivirus vectors inhibit lymphangiogenesis and lymphatic metastasis of breast tumor [29] and gallbladder cancer [30] respectively. Because VEGFR-3 is specifically expressed on LEPCs and mature lymphatic endothelial cells [31], it may be a novel therapeutic RNAi target of inhibiting lymphangiogenesis for reducing tumor metastasis. Further studies are needed to understand effects of PEI-alginate/VEGFR-3 siRNA nanocomplexes on inhibiting tumor lymphangionenesis and lymphatic metastasis of tumor cells.

Our findings provide the first evidence that VEGFR-3 mRNA targeting with siRNA delivery into the cells is effective for inhibiting behaviors of EPC lymphangiogenesis. Antibodies to VEGFR-3 have been applied for targeting inhibition of VEGFR-3 signaling. Systemic administration of monoclonal antibody to VEGFR-3 prevents lymphangiogenesis in skin healing and breast cancer models [32]. Inhibition of VEGFR-3 activation with specific antagonist antibodies suppresses lymphangiogenesis and metastasis to regional lymph nodes and lungs [33]. Blockade of VEGFR-3 by monoclonal antibodies reduces tumor lymphangiogenesis, lymphatic metastasis and lung metastasis [34]. However, antibodies to VEGFR-3 may cause immune reaction in systemic administration. Moreover, soluble VEGFR-3 expressed in adenovirus, which blocks VEGFR-3 signaling through binding VEGF-C and VEGF-D, is effective for inhibiting tumor lymphangiogenesis and lymphatic metastasis [35–37]. Intravenous administration of adenoviruses expressing soluble VEGFR has been shown to cause severe side effects [38]. Therefore, VEGFR-3 mRNA targeting with PEI-alginate/siRNA nanocomplexes will be an effective strategy for inhibiting tumor lymphangiogenesis.

Data in this study show that PEI-alginate nanoparticle is a useful vector for efficient loading and cytoplasmic delivery of VEGFR-3 siRNA. PEI is an organic molecule with a high cationic charge-density potential based on the presence of multiple amino groups within its backbone, and can spontaneously adhere to and condense siRNA to form toroidal nanoparticles [39]. PEI nanoparticles are easily internalized into the cells by electrostatic interaction between their positive changed polymer and negative charged cell membrane and by cell endocytosis. PEI has buffering capacity to pump additional protons into the lysosome along with the concurrent influx of Cl$^-$ to maintain charge neutrality. Finally, increase of ionic strength causes swelling and rupture of the lysosome, resulting in the escape of siRNA from the degradation in lysosome [40, 41]. Under the culture conditions of our experiments, some PEI-alginate/siRNA nanocomplexes are phagocytized by the cells at 2 h, most nanocomplexes enter the cells at 4 h, and some nanocomplexes are degraded at 6 h after addition into the medium. PEI (25 kDa) nanoparticles may induce membrane damage and initiate apoptosis [42]. Cytotoxicity of PEI is attributed to terminal-NH$_2$ groups and multiple cationic charges. Alginate, a linear anionic polysaccharide, has been used as a safe material for DNA delivery [43, 44]. It can reduce PEI toxicity by neutralizing positive charge of PEI. Cell toxicity of PEI (25 kDa)-alginate (4.8%) nanoparticles is almost negligible, the nanocomposite displays higher efficiency for DNA and siRNA transfection [24]. In our experiments, cytotoxicity of PEI-alginate nanoparticles is lower than PEI nanoparticles in delivering VEGFR-3 siRNA. When N/P ratio is 16, siRNA loading in PEI-alginate nanoparticles is desirable, while toxicity of the nanoparticles is not obvious. These results indicate that alginate may reduce greatly PEI cytotoxicity. When PEI-alginate nanoparticles are bound to VEGFR-3 siRNA, their positive charge on the surface is decreased. The mean charge and size of PEI-alginate/siRNA nanocomplexes (N/P = 16) are 7.56 mV and 139.1 nm respectively. Recently, PEI/siRNA complexes have been administrated systemically or locally at animal disease models [44]. The focus of future work should be to define distribution and degradation of PEI-alginate/siRNA nanocomplexes in tumors.

In summary, VEGF-C/VEGFR-3 signaling pathway is involved in differentiation and lymphangiogenesis of CD34$^+$VGFR-3$^+$ EPCs. VEGFR-3 implies as a potential target for inhibiting tumor lymphangi-

ogensis. PEI-alginate nanoparticle is effective vector for delivering VEGFR-3 siRNA. Delivery of VEGFR-3 siRNA with PEI-alginate nanoparticles may be a potential therapy for inhibiting tumor lymphangiogensis and suppressing lymphatic metastasis and graft rejection.

Acknowledgments

Competing Interests

The authors have declared that no competing interest exists.

References

1. Detry B, Bruyere F, Erpicum C, et al. Digging deeper into lymphatic vessel formation in vitro and in vivo. BMC Cell Biology. 2011; 12: 29.
2. Tan Y. Basic fibroblast growth factor-mediated lymphangiogenesis of lymphatic endothelial cells isolated from dog thoracic ducts: effects of heparin. Jap J Physiol. 1998; 42: 133–41.
3. Jussila L, Alitalo K. Vascular growth factors and lymphangiogenesis. Physiol Rev. 2002; 82: 673–700.
4. Avraamides CJ, Garmy-Susini B, Varner JA. Integrins in angiogenesis and lymphangiogenesis. Nat Rev Cancer. 2008; 8: 604–17.
5. Paupert J, Sounni NE, Noël A. Lymphangiogenesis in post-natal tissue remodeling: lymphatic endothelial cell connection with its environment. Mol Aspects Med. 2011; 32: 146–58.
6. Alitalo K. The lymphatic vasculature in disease. Nat Med. 2011; 17: 1371–80.
7. Schulte-Merker S, Sabine A, Petrova TV. Lymphatic vascular morphogenesis in development, physiology, and disease. J Cell Biol. 2011; 193: 607–18.
8. Al-Rawi MAA, Jiang WG. Lymphangiogenesis and cancer metastasis. Front Biosci. 2011; 16: 723–39.
9. Wigle JT, Oliver G. Prox1 function is required for the development of the murine lymphatic system. Cell. 1999; 98: 769–78.
10. Kreuger J, Nilsson I, Kerjaschki D, et al. Early lymph vessel development from embryonic stem cells. Arterioscler Thromb Vasc Biol. 2006; 26: 1073–8.
11. Salven P, Mustjoki S, Alitalo R, et al. VEGFR-3 and CD133 identify a population of CD34+ lymphatic/vascular endothelial precursor cells. Blood. 2003; 101: 168–72.
12. Bogos K, Renyi-Vamos F, Dobos J, et al. High VEGFR-3-positive circulating lymphatic/vascular endothelial progenitor cell level is associated with poor prognosis in human small cell lung cancer. Clin Cancer Res. 2009; 15: 1741–6.
13. Nguyen VA, Furhapter C, Obexer P, et al. Endothelial cells from cord blood CD133+CD34+ progenitors share phenotypic, functional and gene expression profile similarities with lymphatics. J Cell Mol Med. 2009; 13: 522–34.
14. Religa P, Cao R, Bjorndahl M, et al. Presence of bone marrow-derived circulating progenitor endothelial cells in the newly formed lymphatic vessels. Blood. 2005; 106: 4184–90.
15. Kerjaschki D, Huttary N, Raab I, et al. Lymphatic endothelial progenitor cells contribute to de novo lymphangiogenesis in human renal transplants. Nat Med. 2006; 12: 230–4.
16. Schniedermann J, Rennecke M, Buttler K, et al. Mouse lung contains endothelial progenitors with high capacity to form blood and lymphatic vessels. BMC Cell Biol. 2010; 11: 50.
17. Kim DH, Rossi JJ. Strategies for silencing human disease using RNA interference. Nat Rev Genet. 2007; 8: 173–84.
18. Pecot CV, Calin GA, Coleman RL, et al. RNA interference in the clinic: challenges and future directions. Nat Rev Cancer. 2011; 11: 59–67.
19. Beloor J, Choi CS, Nam HY, et al. Arginine-engrafted biodegradable polymer for the systemic delivery of therapeutic siRNA. Biomaterials. 2012; 33: 1640–50.
20. Schiffelers RM, Ansari A, Xu J, et al. Cancer siRNA therapy by tumor selective delivery with ligand-targeted sterically stabilized nanoparticle. Nucleic Acids Res. 2004; 32: e149.
21. Wang HJ, Zhang D, Tan YZ, et al. Autophagy in endothelial progenitor cells is cytoprotective in hypoxic conditions. Am J Physiol Cell Physiol. 2013; 304: C617–26.
22. Wu JH, Wang HJ, Tan YZ, et al. Characterization of rat very small embryonic-like stem cells and cardiac repair after cell transplantation for myocardial infarction. Stem Cells Dev. 2012; 21: 1367–79.
23. Wang HJ, Tan YZ, Zhang MH, et al. Vascular endothelial growth factor-C-induced differentiation of CD34+CD133+VEGFR-3+ EPCs towards lymphatic endothelial cells. Jpn J Lymphology. 2005; 28: 71–3.
24. Patnaik S, Arif M, Pathak A, et al. PEI-alginate nanocomposites: efficient non-viral vectors for nucleic acids. Int J Pharmaceut. 2010; 385: 194–202.
25. Zhang DY, Wang HJ, Tan YZ. Wnt/β-catenin signaling induces the aging of mesenchymal stem cells through the DNA damage response and the p53/p21 pathway. PLoS ONE. 2011; 6: e21397.
26. Guo HD, Wang HJ, Tan YZ, et al. Transplantation of marrow-derived cardiac stem cells carried in fibrin improves cardiac function after myocardial infarction. Tissue Eng Part A. 2011; 17: 45–58.
27. Waseem NH, Lane DP. Monoclonal antibody analysis of the proliferating cell nuclear antigen (PCNA). Structural conservation and the detection of a nucleolar form. J Cell Sci. 1990; 96: 121–9.
28. Norrmén C, Tammela T, Petrova TV, et al. Biological basis of therapeutic lymphangiogenesis. Circulation. 2011; 123: 1335–51.
29. Chen Z, Varney ML, Backora MW, et al. Down-regulation of vascular endothelial cell growth factor-C expression using small interfering RNA vectors in mammary tumors inhibits tumor lymphangiogenesis and spontaneous metastasis and enhances survival. Cancer Res. 2005; 65: 9004–11.
30. Lin W, Jiang L, Chen Y, et al. Vascular endothelial growth factor-D promotes growth, lymphangiogenesis and lymphatic metastasis in gallbladder cancer. Cancer Lett. 2012; 314: 127–36.
31. Kaipainen A, Korhonen J, Mustonen T, et al. Expression of the fms-like tyrosine kinase 4 gene becomes restricted to lymphatic endothelium during development. Proc Natl Acad Sci USA. 1995; 92: 3566–70.
32. Pytowski B, Goldman J, Persaud K, et al. Complete and specific inhibition of adult lymphatic regeneration by a novel VEGFR-3 neutralizing antibody. J Natl Cancer Inst. 2005; 97: 14–21.
33. Roberts N, Kloos B, Cassella M, et al. Inhibition of VEGFR-3 activation with the antagonistic antibody more potently suppresses lymph node and distant metastases than inactivation of VEGFR-2. Cancer Res. 2006; 66: 2650–7.
34. Burton JB, Priceman SJ, Sung JL, et al. Suppression of prostate cancer nodal and systemic metastasis by blockade of the lymphangiogenic axis. Cancer Res. 2008; 68: 7828–37.
35. Lin J, Lalani AS, Harding TC, et al. Inhibition of lymphogenous metastasis using adeno-associated virus-mediated gene transfer of a soluble VEGFR-3 decoy receptor. Cancer Res. 2005; 65: 6901–9.
36. He Y, Kozaki K, Karpanen T, et al. Suppression of tumor lymphangiogenesis and lymph node metastasis by blocking vascular endothelial growth factor receptor 3 signaling. J Natl Cancer Inst. 2002; 94: 819–25.
37. Yang H, Kim C, Kim MJ, et al. Soluble vascular endothelial growth factor receptor-3 suppresses lymphangiogenesis and lymphatic metastasis in bladder cancer. Mol Cancer. 2011; 10: 36.
38. Mahasreshti PJ, Kataram M, Wang MH, et al. Intravenous delivery of adenovirus-mediated soluble FLT-1 results in liver toxicity. Clin Cancer Res. 2003; 9: 2701–10.
39. Goldsmith M, Mizrahy S, Peer D. Grand challenges in modulating the immune response with RNAi nanomedicines. Nanomedicine. 2011; 6: 1771-85.
40. Akinc A, Thomas M, Klibanov AM, et al. Exploring polyethylenimine-mediated DNA transfection and the proton sponge hypothesis. J Gene Med. 2005; 7: 657–63.
41. Moghimi SM, Symonds P, Murray JC, et al. A two-stage poly(ethylenimine)-mediated cytotoxicity: implications for gene transfer/therapy. Mol Ther. 2005; 11: 990–5.
42. Padmanabhan K, Smith TJ. A preliminary investigation of modified alginates as a matrix for gene transfection in a HeLa cell model. Pharm Dev Technol. 2002; 7: 97–101.
43. Higashi T, Nagamori E, Sone T, et al. A novel transfection method for mammalian cells using calcium alginate microbeads. J Biosci Bioeng. 2004; 97: 191–5.
44. Günther M, Lipka J, Malek A, et al. Polyethylenimines for RNAi-mediated gene targeting in vivo and siRNA delivery to the lung. Eur J Pharm Biopharm. 2011; 77: 438–49.